Functional analysis of plant organ development with sub-cellular resolutions.

Running title: Quantitative plant cell biology in situ.

ABSTRACT

Given the rapid development of plant genetic engineering, a lack of precise plant phenotyping methods at cellular resolution limits our ability to dissect the genetic/epigenetic origin of quantitative traits on whole organ level and our ability to link gene function, expression, localization with phenotype.

Here we describe an effective, high-resolution phenotyping platform that allows the detection of organ and cell shapes, quantified gene expressions, chromatin organization, cell cycle kinetics, cell polarity, and protein-protein interactions at subcellular resolution. The platform is marker-free and plant-species independent. The platform has been tested for the analysis of diverse organs in several plant species, including grasses. The platform's application requires minimal time and experience from researchers and can be completed in 3-4 working days (including complete data extraction for each cell). The method require high-resolution microscopy and state of art computer. We present the results of platform applications in diverse developmental contexts. The platform is free and open-source, with a user-friendly graphical interface.

Introduction.

A large-scale quantitative study of cell shape and cell functionality in multicellular organs entails an accurate estimation of the quantitative three-dimensional geometry and functions of each cell in an organ (Bassel, G. W., 2019). State-of-the-art confocal and other similar microscopes allow researchers to scan 3-D images after specific labeling of cell boundary, chromatin, detect cell cycle events and proteins localization after to high-resolution volumetric images acquisition for almost all plant organs (Rowland, R. E., & Nickless, E. M., 2000). Spatial position, orientation and volume of cells comprising an organ are attractive candidate parameters to characterize mutant’s phenotypes or gene-editing effects.

Recently developed methods allow performing precise segmentation based on cell border labeling (Liu et al., 2014). This approach, combined with the detection of nuclei and cell cycle events (Schulz et al., 2006; Pasternak et al., 2017), allows us to perform simultaneous analysis of cell geometry, cell cycle duration and the geometry of organelles. Cell positions within organs are defined using an internal organ coordinate system based on the position of organ tip (QC in the root). Cell boundary labeling enables integration of multiple cell types into organ/organelle atlases with pre-

cise description of cellular neighborhoods.. A recently developed technique will allow us to perform quantitative gene expression analysis (Omeljanchuk et al., 2016) and localization and quantification of the protein complex (Pasternak et al., 2018). All these approaches, including protocols for plant organ labeling, image scanning, processing, layer identification, and analysis, were integrated into the High-Resolution Plant Phenotyping Platform (HRPPP), a deep pipeline for volumetric segmentation and analysis of the geometry of plant tissue, detection and quantitative analysis of cell cycle events, chromatin status, gene expression and protein complex at cellular resolution. The platform's main advantages are the ability to analyze cell volume and simultaneously tracking all cells in organs with its connections. The platform's main advantages over widely used MorhoGraphX are the possibility to combine multichannel/multigene process analysis like cell geometry, cell cycle kinetics, and gene expression in the same cells.

The platform does not require markers; hence it can be applied for diverse plant species.

Experimental design:

The pipeline includes growing plants *in vitro* or in soil, incubation with 5-ethynyl-2′-deoxyuridine (EdU) for cell cycle kinetics or other chemicals according to the task, tissue fixation, labeling, scanning, and image processing.

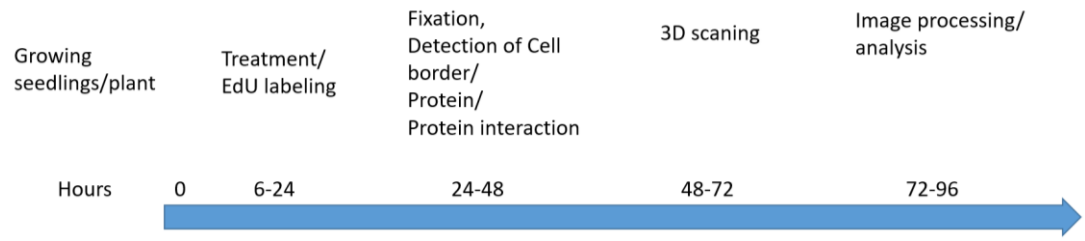

Figure 1. Pipeline step by step with timing (in hours). The whole procedure from treatment to full extraction of the data required less as 96 hours.

Labelling methods and parameters extracted.

The platform includes four different tissue labeling options or its combinations: cell border labelling, nuclei labeling (including EdU labeling for cell cycle kinetics), gene expression (protein localization), and protein complex detection. All four options can be combined to study cell geometry/cell cycle/gene expression simultaneously. Since the quality of labeling is crucial for further analysis, we will describe the procedure in detail in the next part. Obtaining the required very high quality images is very chal-

lenging, therefore we describe the most important aspects in detail and give protocols in the upcoming sections.

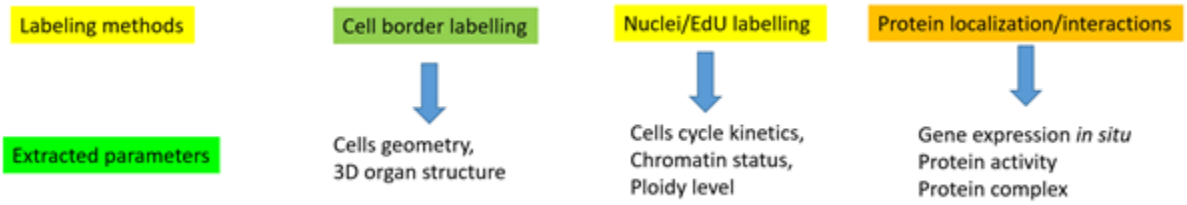

Figure 2. Labeling options.

Comparison with other methods:

Staining methods.

There are several staining methods for cell border visualization. However, for automatic image analysis special care must be taken. Namely, cell border thickness along whole organs must be uniform for equal cell border detection. Also, living objects (especially root), were hard to label and scan because or rapid growth and movement. The analysis of whole organs at sub-cellular resolution requires recording multiple tiles (typically 3-5), with depth-dependent dynamic adaption of recording parameters. So, although the pipeline does not preclude live imaging, high quality analyses can only be performed on fixed tissue.. How to detect cell boundaries? With plant cells there are two options: cell wall and plasma membrane.

One of the necessary conditions for boundary detection is the equal intensity of the boundary of each cell. Simple cellulose labeling is not suitable for boundary label and detection, due to the variation of cell wall thickness and other cell wall properties within an organ.

We made optimization of the cell wall labelling by partial digestion of cell wall what allow us to make almost equal signal intensity from all cell layers after calofluor white labelling. This labelling can be combined with nuclei detection, gene expression analysis by immunolocalization, PLA assay.

The second possibility is to use polysaccharide labelling after normalization of ketone bound digestion (pseudo-Schiff reagent). However, this labelling requires pH 1,4 and can not be combined with any other labelling.

One of the simplest decisions is to use the plasma membrane as a target marker: this should give us an almost equal label for all cell files. FM™ 4-64FX as a fixable analogy of FM™ 4-64 membrane stain has been tested for double/triple labeling.

We have found that gentle fixation procedure allows us to get satisfactory segmentation quality. However, it does not allow us to get good DAPI or antibody labeling. A more vigorous fixation procedure punctuated the membrane lipid bilayers.

Software for image analysis:

MorphoGraphX (MGPX) software has been developed for 3D/4D segmentation of plant organ (de Reuille *et al*., 2015; http://www.MorphoGraphX.org) as an analog of previously published iRoCS (Schmidt et al., 2014) and allowed to extract cell geometry. Software has been used in numerous publications for analysis of organ geometry (Kierzkowski, D. et al., 2019; Kierzkowski, D., & Routier-Kierzkowska, A. L. (2019). Zhu, M., et al., 2020). However, MorphopgrahX does not allow us to analyze cell cycle kinetics, gene expression, and protein complex. Moreover, contrary to ours, it does not allow us to perform fully manual corrections, only by changes segmentation options. Layers labeling options are also missing and should be done based on organ morphology.

Limitations of the platform:

The platform can be applied tofor the majority of the plant organs. However, thick organs (more than 500 µm thickness) may require longitudinal sections before processing/scanning.

Materials and method.

REAGENTS and EQUIPMENT

Equipment.

Microscope.

Any confocal or other microscopes which allow to scan 3D images with high resolution. For thick objects we recommend to use a 2-photon microscope.

Computer.

Software requires computer with minimal RAM size 16 Gb (64GB for high resolution segmentation recommended).

Plant material preparation and labelling.

Plants of *Arabidopsis thaliana*, *Nicotiana tabacum*, *Setaria Italica*, and *Lycopersicum esculentum* have been used. All procedures of plant cultivation, fixation, treatments, imaging was essential as described previously (Pasternak et al., 2015, Pasternak et al., 2017; Pasternak et al., 2020).

Our cell boundary labelling protocol is based on binding of propidium iodide to deketonized polysaccharides of the cell wall under low pH (1,4) in the presence of

sulfur. Although basic protocol has been described previously, significant modifications are required to adapt the protocol for 3D scanning and analysis. Namely, fixation in acetic acid led to significant tissue maceration and often damaged the more soft mature part. That's why we recommend performing fixation with formaldehyde in MTSB buffer at pH 7. The de-ketonization level (time of periodic acid treatment) is another crucial parameter. For Arabidopsis root 30 minutes, de-ketonization in 1% periodic acid partially punctuated the cell walls especially in the mature part. We recommend reducing de-ketonization time to 15-20 minutes. Mounting procedure is another crucial step. One has to use a spacer with a thickness similar to your object (100 µm for Arabidopsis root, 300 µm for tobacco root). For thin object, one can use double-side scanning by mounting samples between 2 coverslips: 24x60 as base and 24x32 as cover. This adjustment allows scanning objects from both sides to avoid low signal/noise ratio in the down part.

Scanning procedure.

Note: Always adjust immersion medium and embedding medium to the average refractive index of the sample for optimum image quality especially for deep optical sectioning.

A confocal laser scanning miscroscope with at least four lasers (2P, 488, 543/561, and 633) are required. We recommend the following objectives: x25 for cell geometry with glycerol immersion and x40 or x63 for gene expression, cell cycle, and chromatin structure analysis.

Scanning should be performed with at least 1024x1024 pixels per frame at 16Bit and with amplifier offset close to zero to avoid underexposed image regions. Z-stack corrections are highly recommended to obtain reasonable SNR throughout the stack while avoiding over-exposure. To increase image quality in the down part, one can increase average numbers or reduce scanning speed in this region. Choice of the optimal objective depends on the type of analysis: for cell volumetric analysis x25 or x40 objective with immersion correction should be used. For gene expression analysis, cell cycle analysis and chromatin structure, minimum x40, but better x63 objective should be used.

Image processing and data extraction pipeline.

A detailed tutorial was presented in supplemental materials.

Anticipated results.

Below we demonstrated application of the platform for diverse plant organ and species.

1.Volumetric root analysis.

As the most straightforward platform applications option, we perform a quantitative analysis of Arabidopsis root apical meristem geometry with 3D resolution. Evaluation of cell elongation and cell volume in each cell continuity in each file were performed.

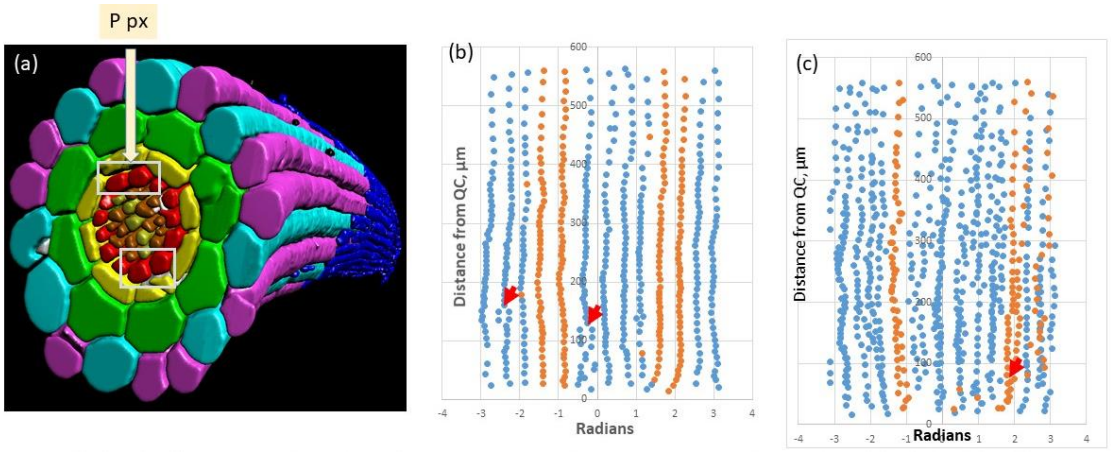

Figure 3.

Analysis of cell geometry in 5 days old root tissues. (a) – root render. Color code: trichoblast is in blue; atrichoblast is in magenta; Cortex is in green; endodermis is in yellow; pericycle is in red; stele in is brown with phloem is in dark-yellow; (b)- virtually unrolled pericycle: orange circle- protoxylem pole pericycle cells. (c)

Virtually unrolled vasculature. Xylem is in orange. Red arrows show periclinal cell positions in pericycle and xylem. Dots represent cell's center positions projected to dimensions angle (in radians, x-axis) and distance from QC along the root's axis (y-axis).

Growth can be determined as changes in volume (not length); that's why we compare changes in the length and volume for inner and outer cell layers: epidermis and pericycle. Figure 4 demonstrates differences in cell growth in inner and outer cell layers. The 3D analysis allows us to distinguish between the geometry of different pericycle and epidermis cell subtypes. Both cell types are heterogeneous tissue with two different populations—namely, trichoblast and atrichoblast in epidermis and xylem pole and phloem pole in pericycle. To further extend the analysis, we quantified the volume of both pericycle cell types.

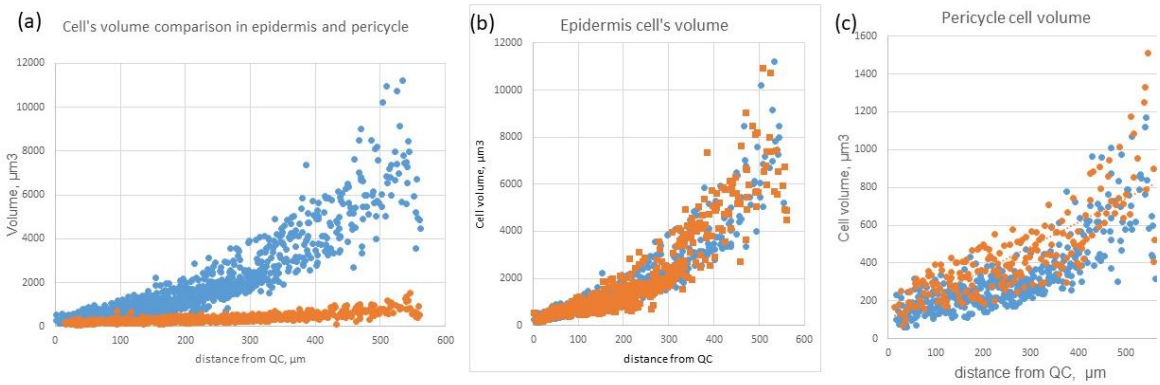

Figure 4. (a) – comparison of cell volume distribution along the axis in different cell files Blue- epidermis; Orange – pericycle. (b)-epidermis cells: atrichoblast (blue) vs trichoblast (orange); (c) Pericycle cells: – protoxylem pole cell (orange) and rest (blue). Note differences in scale between (b) and (c).

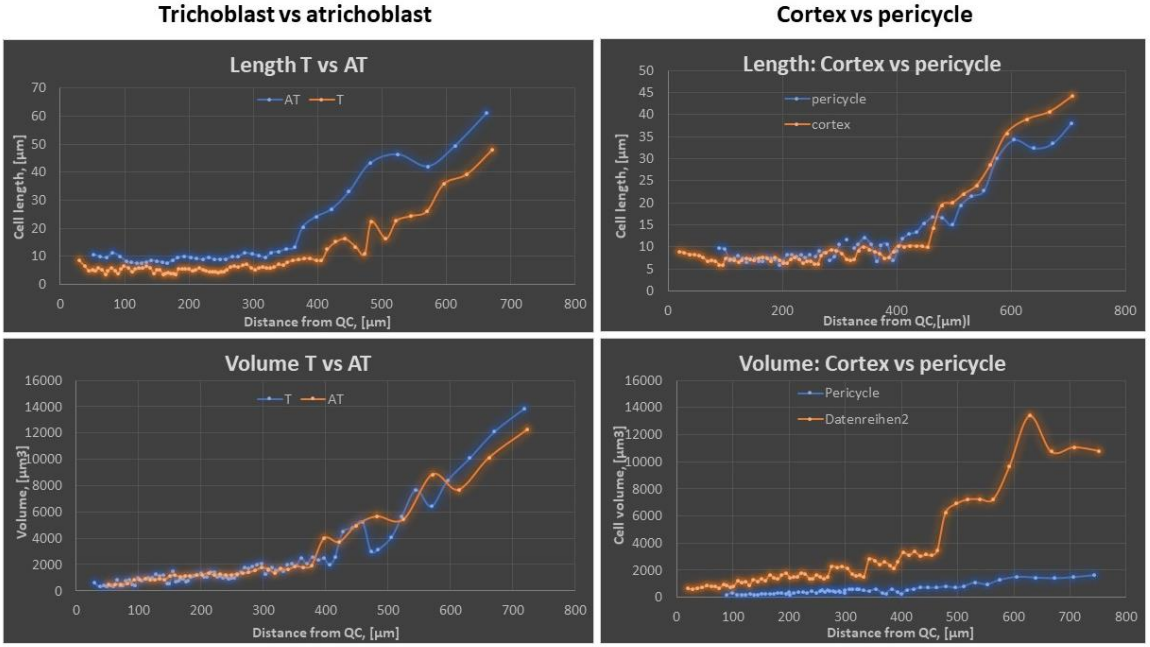

Figure 5. Comparison cell growth and cell elongation in different cell files. T and AT have the same volume, but AT cells are two times longer in axial direction.
There are no differences in pericycle and cortex length, but cortex are 15 times bigger (volume) as pericycle.

The next important root feature that can determine precisely quantified is “root regularity”- orientation of cell division (polarity of cell division). In Arabidopsis, the root direction of cell division/cell polarity occurred towards root growth, mainly anticlinal. Tangential and periclinal cell divisions indicate defects in the polarity of the division

plate. Wild type roots under control conditions have a very regular structure with only a few periclinal/tangential cell divisions.

Irregular cell division orientation occurred in the epidermis and endodermis. In both cases, cell fate changed after such division: (T-AT in the epidermis and middle cortex/endodermis in the endodermis).

Level of cell orientation irregularity was significantly increasing after treatment with fungal toxin Brefeldin A. We demonstrated the application of our pipeline for investigation of the phenomena of irregularity of root structure. An example is shown in figure 6.

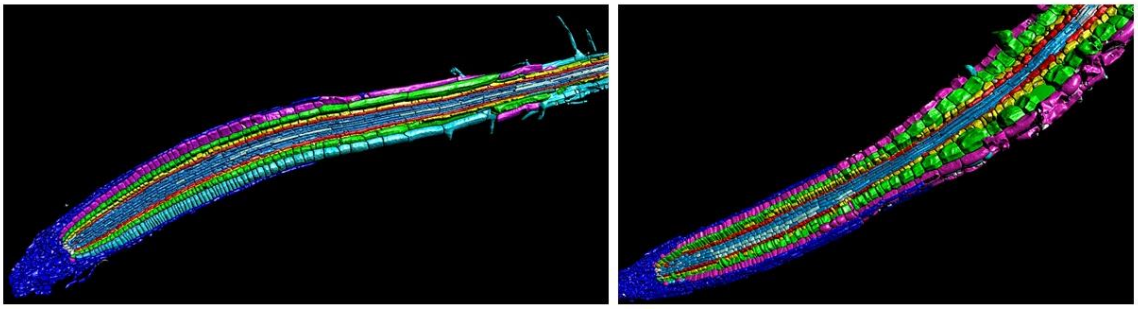

Figure 6. Seedlings have been treated with 10 µM BFA for 24 hours. Root has been scanned, segmented and layers were assigned. Trichoblast is in blue, atrichoblast is in magenta; cortex is in green; endodermis is in yellow; pericycle is in red; stelle is in middle-blue/xylem is white-blue. (a) – control; (b) – treatment with 10 µM BFA for 24 hours.

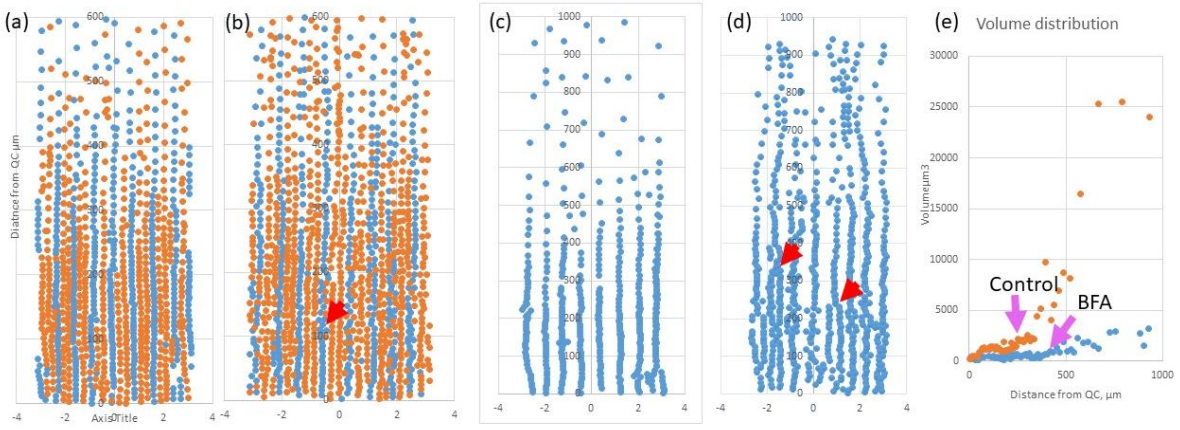

Figure 7. (a,b) – Positions of each cell in epidermis (a-control; b- BFA); cortex (c – control; d- BFA) in virtually unrolled root; (e) –distribution of the cell volume in the cortex cell. Orange – control; blue- BFA.

Defects in cell polarity reflected by periclinal and tangential cell division in epidermis and cortex were quantified (arrows on panels b, d). Geometrical meristem length after BFA treatment was extended (panel e)

In figure 7, we provide a quantitative analysis of root irregularity. It was shown that BFA mainly induces abnormality in the inner cell layers, including switching between trichoblast and atrihoblast cell files and increasing number of cortex cell files by induction of tangential cell divisions. Numbers and positions of tangential divisions are shown in the virtually unrolled root. Despite cortex cells showing significant lateral expansion in the elongation zone, this expansion can't compensate changes in cell volume by elongation as shown on panel d.

Next, we tested the possibility of quantifying root structure in the other species as monocot C4 plants.

Quantitative analysis of lateral organs.

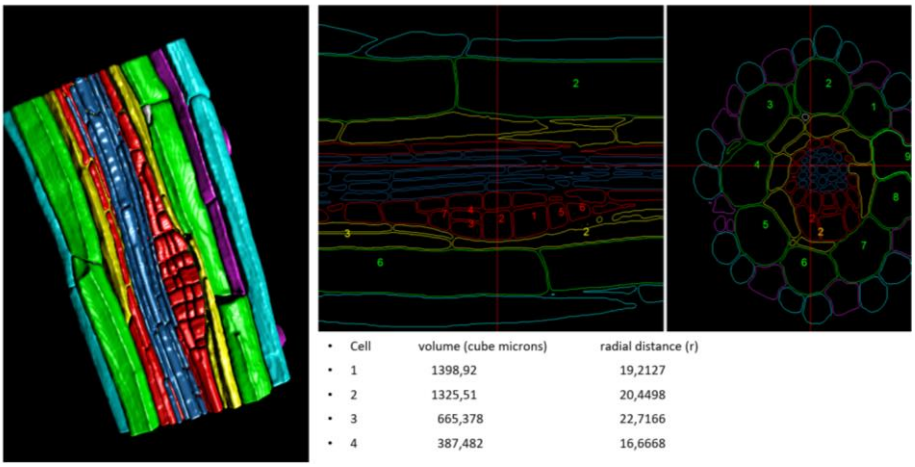

Cell	volume (cube microns)	radial distance (r)
1	1398,92	19,2127
2	1325,51	20,4498
3	665,378	22,7166
4	387,482	16,6668

Supplementary figure. Lateral root was segmented, layers labelling, and quantitative data were extracted. Cell volume of 4 cells were shown as an example. Pericycle/lateral root are in red.

Protocol application for the large roots.

The protocol allows to get quantitative root analysis of Tobacco and Millet with root diameter up to 300 µm (figure 8, 9).

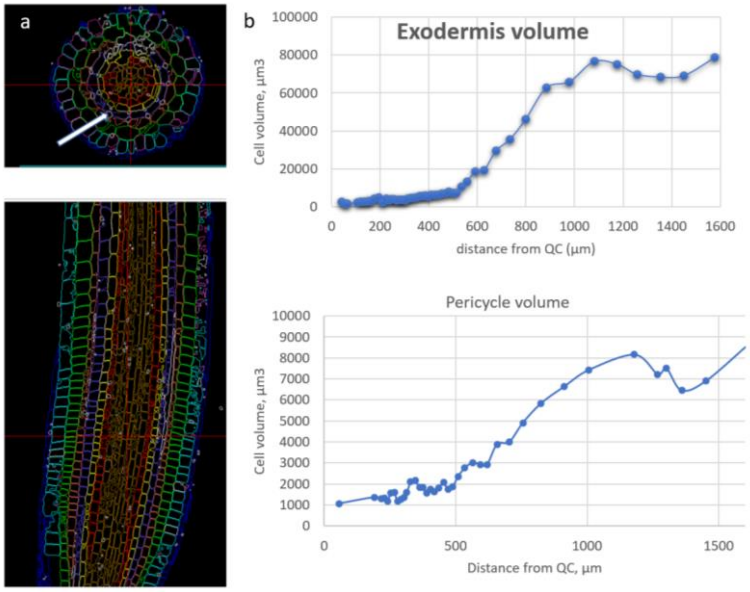

Figure 8. Tobacco root analysis. (a) . Segmented and assigned tobacco root. „Holes“ aerenchyma between cortex2 and cortex3 and between cortex 3 and endodermis shown by white arrow.

(b)- Evolution of cell volume of exodermis and pericycle along the axis.

Notes: 10 times differences in volume scale bar between exodermis and pericycle.

As conclusion, polysaccharide labelling allows to investigate quantitative root geometry because provide equal labelling intensity to all cells file, independently from cellulose contents in cell wall.

2. Functional root analysis.

In order to perform analysis of cell cycle kinetics, cell cycle duration, chromatin status, and gene expression, we combined a general nuclear label (DAPI) with immunolocalization or detection of DNA replication marker.

Several tasks have been addressed by combining gene expression investigations, cell cycle kinetics, and protein complex abundance integrated into the platform pipeline.

One essential finding is that root zonation is cell type/subtype specific. Previously root zonation was defined on changes in Cortex cell length which only very roughly approximates reality.

Root zonation based on cell cycle/endocycle maps.

The determination of root zonation is a great challenge in plant biology.

There are several criteria that have been suggested for the determination of root zones.

The majority of the root zonation model is based on the assumption of equal cell elongation in all cell files. Commonly used measurements based on the cortex cell's linear size (elongation) (for Arabidopsis) has been considered a criterium of determination of proliferation domain. However, this criterium does not link with real proliferation activities and considers small cells that are not elongated as meristemic. Moreover, one has to consider the fact that cell layers in the root have bilateral, but not radial symmetry with different cell linearity even from the same cell type (endodermis, pericycle) having different cell cycle distribution in the proliferation zone. The most interesting question is about proliferation activity in inner cell layers (xylem/phloem and vasculature).

Our platform allows researchers to quantify the length of proliferation (cell proliferation activity) and transition (endocycle activity) domain length for each cell type and sub-type based on direct detection of mitotic events and endocycle events.

We can also perform precise zonation and create a map of each layer of the distal meristem (columella and each layer of lateral root cap) with determination proliferation and transition domain length and quiescence (G1 duration in QC).

We applied these protocols for quantifications of domain length in Arabidopsis (including several mutants and overexpression line 35S::WOX5), tobacco, and tomato roots.

Below we show some examples—determination of proliferation and transition zones in Arabidopsis thaliana root.

.

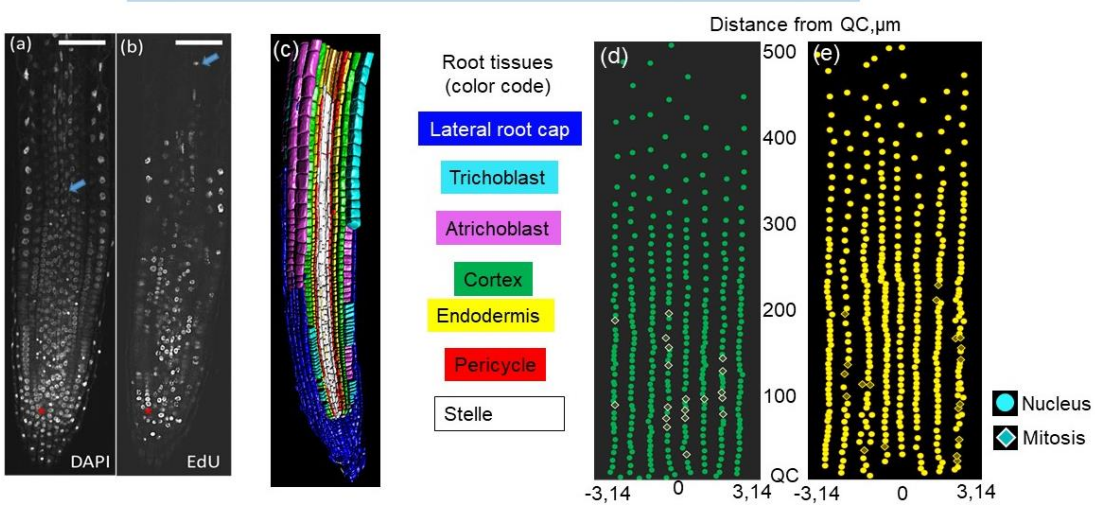

Figure 10. Annotation of mitosis and DNA replication in A. thaliana.

(a) – The root tip staining with DAPI for annotation of the nuclei positions and mitosis distributions. (b) – EdU-incorporated nuclei in the same root tip were an-

notated to study DNA replication events. Bars 50 µm. (c) -root with color code; (d), (e) – mitosis map of a virtually “unrolled” cortex (d) and endodermis (e) layers of A. thaliana root tip. From Lavrekha et al., 2017.

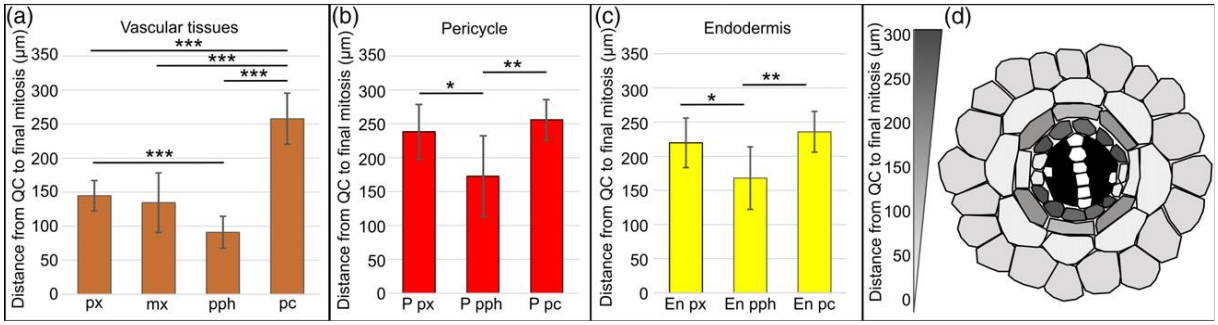

Figure 11. Length of proliferation zones in different cell sub-types in wild-type Arabidopsis root. Length of proliferation zone have been estimated as position of the last mitosis in certain cell file/cell continuity. Our analysis revealed that zone length in endodermis, pericycle and vasculature depend on cell fate/position. From Lavrekha et al., 2017.

We define the transition zone as the zone between the position of the last mitosis and the position of the last DNA replication event. This zone correlated well with slight cell elongation.

As an example of platform application we investigate effect of sucrose and light on proliferation and transition zone length in Arabidopsis root.

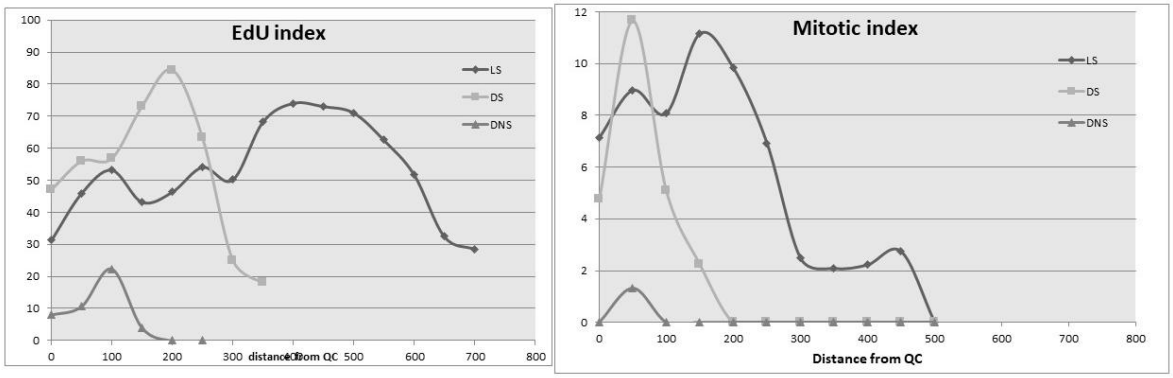

Figure 12: Arabidopsis seedling have been incubated for 36 hours under light or dark conditions with or without sucrose. EdU has been added for 90 minutes. EdU and mitotic index were determined for each 50 µm virtual root segments. Epidermis from typical root were shown. EdU and mitotic index were calculated by dividing the number of cells passing DNA replication or mitosis to total number of cells in each segment. Legends: LS- light + sucrose; DS- dark + sucrose; DNS dark no sucrose.

Higher EdU-index in transition zone can be explained by shorter endocycle duration to compare with cell cycle.

Cell cycle duration.

Root development is a complex spatial-temporal process in which local differences in cell proliferation frequency play a key role. Namely, stem cell niche was characterized by significant extension of G1 duration what can serve as a “marker of cell quiescence”. The differences in cell growth kinetics between different cell files in Arabidopsis RAM led us to the hypothesis that cell cycle duration is not the same in different cells file as a possible mechanism of keeping root integrity. Understanding local differences between cell cycle duration requires the quantitative estimation of the duration of the mitotic cell cycle phases at every position in each cell file.

However, so far, a precise method for such analysis is missing.

Here, we present a simple and robust method for estimating the duration of critical stages of the cell cycle in all cell layers in a plant’s root. The method combines marker-free experimental techniques with the computational Intrinsic Root Coordinate System (iRoCS) for the analysis of the kinetics of all key events in cell cycle stages.

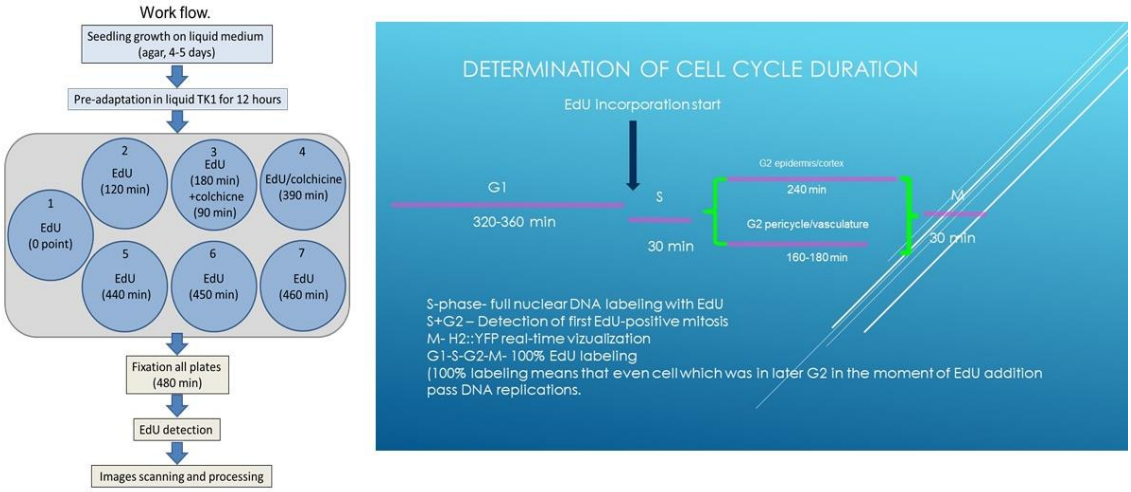

Figure 13. Different EdU/colchicine incubation time has been used as tool for estimating the duration of cell cycle stages. Work-flow of experiment was shown on panel A, while results were briefly described on panel B. Endocycle duration is much shorter compared to cell cycle. Cell cycle duration (in particular G2 duration) is 90 min shorter in stele/pericycle compared to epidermis. S+G2+M duration in Arabidopsis in our conditions is 4 hours in the pericycle and up to 5,5 hours in the epidermis.

Quantification of the chromatin organization/modification in Arabidopsis root

In-plant organ chromatin structures are determined by DNA methylation and histone modifications. Chromatin organization contributes significantly to the regulation of cell fate determination, cell cycle, and gene expression. That's why we include in the platform options allow to quantify a different aspect of epigenetic regulation in situ. Examples of these options were presented in figure 14.

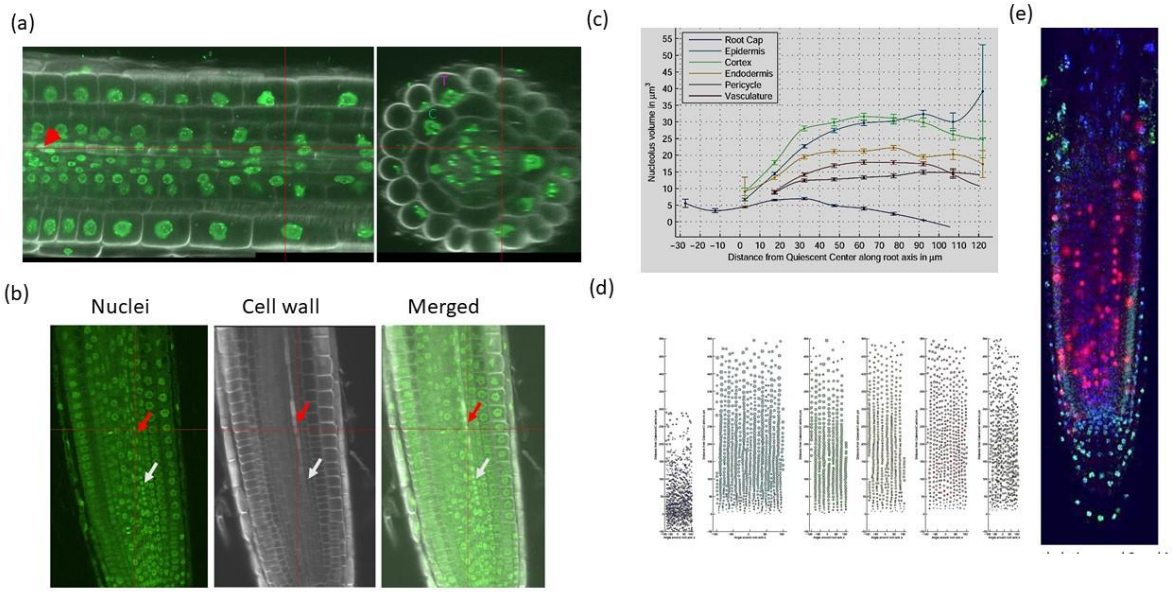

Figure 14.

(a)- cross-section of Arabidopsis root. Nuclei are in green; cell border are in white. Gradient in chromatin landscape from division to elongation zone were shown. T- trichoblast; C- cortex. Red arrow marked condense chromatin in phloem.

(b) – chromatin condensation as a marker of phloem differentiation. Roots have been stained for nuclei (proridium iodide) and for cell wall (Calcofluor white) Cell differentiation in phloem were detected as decrease in nucleolus size and chromatin condensation (white arrow). (c) – average nucleolus volume in different cell files at different distance from QC. (d)- distribution of nucleoli volume in the virtually unrolled root. Circle diameter is proportional to nucleolus volume.

(e) H3K9me2 localization (green) and EdU labelling (red) in Arabidopsis root. H3K9me2 is a marker of heterochromatin abundance.

Functional root analysis of the other species.

To further platform possibility of pipeline application to other root species we performed detailed functional analysis of tobacco root apical meristem (Figure 14, form Pasternak et al., 2017).

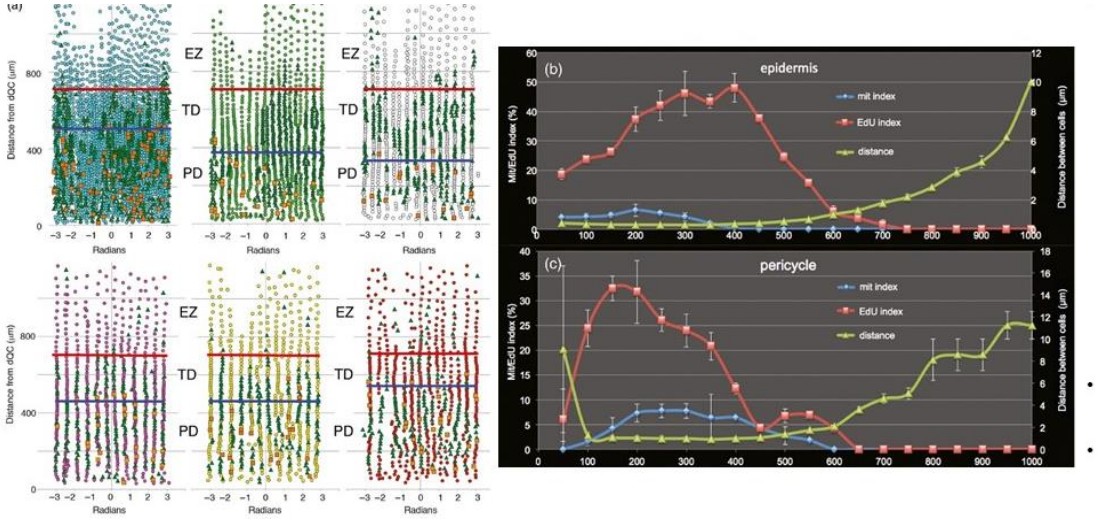

Figure 15. (a) Unrolled cell cylinders for epidermis, cortex1, cortex2, cortex3, endodermis and pericycle cells. EdU-labeled cells are shown as triangles (dark green), mitotic cells as orange squares. In all cell types, the EdU-positive cells extend well beyond the region with mitotic cells. Rapid elongation starts when EdU-positive cells number are declined. Based on the distribution of the mitotic and EdU-positive cells, the root can be divided into a proliferation domain (PD), with DNA replication and mitosis), a transition domain (TD, mainly DNA replication) and an elongation zone (EZ). PD/TD borders: blue horizontal lines, TD/EZ borders: red horizontal lines. X-axis: radians (from −3.14 to 3.14), Y-axis: distance from the QC in μm. (b) Averages of the mitotic and EdU-positive nuclei distributions in the epidermis. (c) Averages of the mitotic and EdU-positive nuclei distributions in pericycle. In each root the number of mitotic and EdU-positive nuclei were calculated per each 50-μm section and normalized to the total cell number in the corresponding section (from Pasternak et al., 2017).

Quantitative analysis of leaf development.

Leaf/SAM is another developing organ with high proliferation activity and with highly complicated structure. The pipeline allows us to perform quantitative analysis of cell geometry, chromatin structure, cell cycle progression, cell differentiation status in leaf/SAM/flowers, and gene expression. Examples of imaging, segmentation, and cell cycle analysis are demonstrated on figure 16.

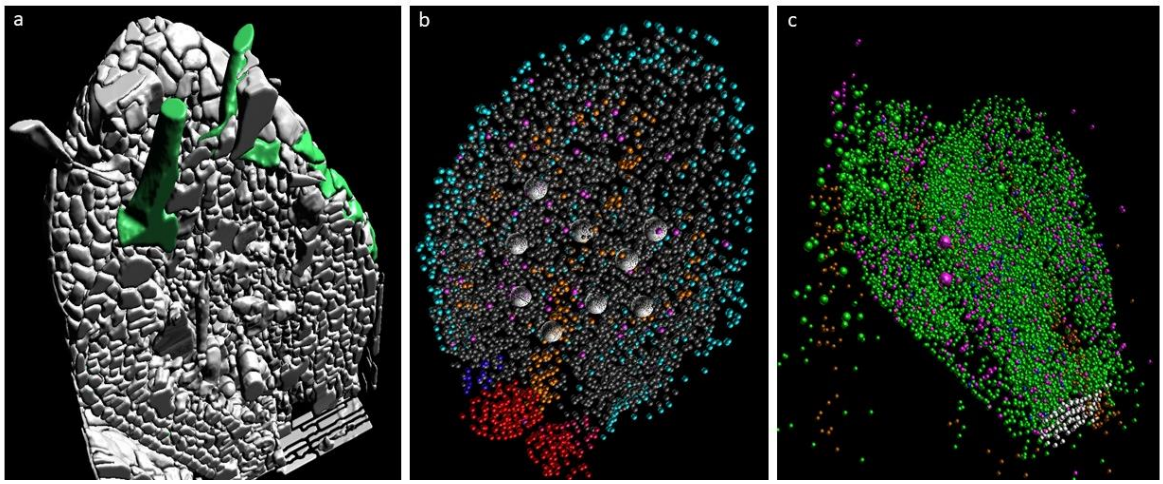

Figure 16. Analysis of cell geometry and cell cycle distribution in Arabidopsis leaf. (a) – cell wall labeling in Arabidopsis SAM: epidermis in in blue, mesophyl cell are in yellow and trichomes are in green.

(b) – nucleus detection in the same organs: epidermis are in blue; SAM are in red; mitotic cells are in magenta;; stipulus are in dark-blue; Vasculature are in brown; mesophyll cells are in grey and trichomes are in white. Note: size of the nuclei in trichomes reflected high ploidy level (c)- Cell cycle activity in leaf/SAM. Seedlings were incubated with EdU for 45 minutes, labelled and processed. Cell are in green; SAM are in white; EdU-positive are in magenta; mitotic cell is in dark-blue; Vasculature are in brown.

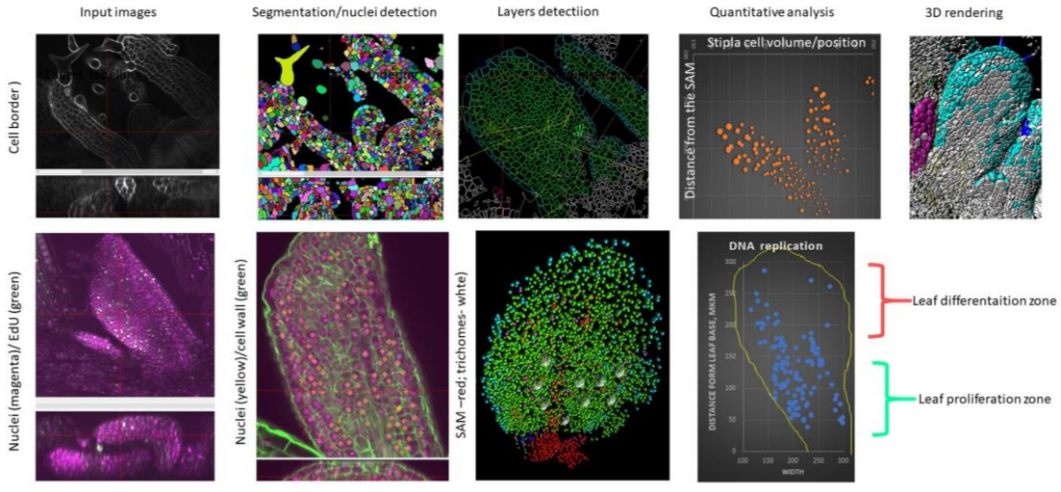

Figure 17. Qiantitative analysis of Arabidopsis SAM.
7 days old shoot were staining for polysaccharide, nuclei, EdU, segmented and analyzed. Position of each of 32000 cells including volume have been extracted.

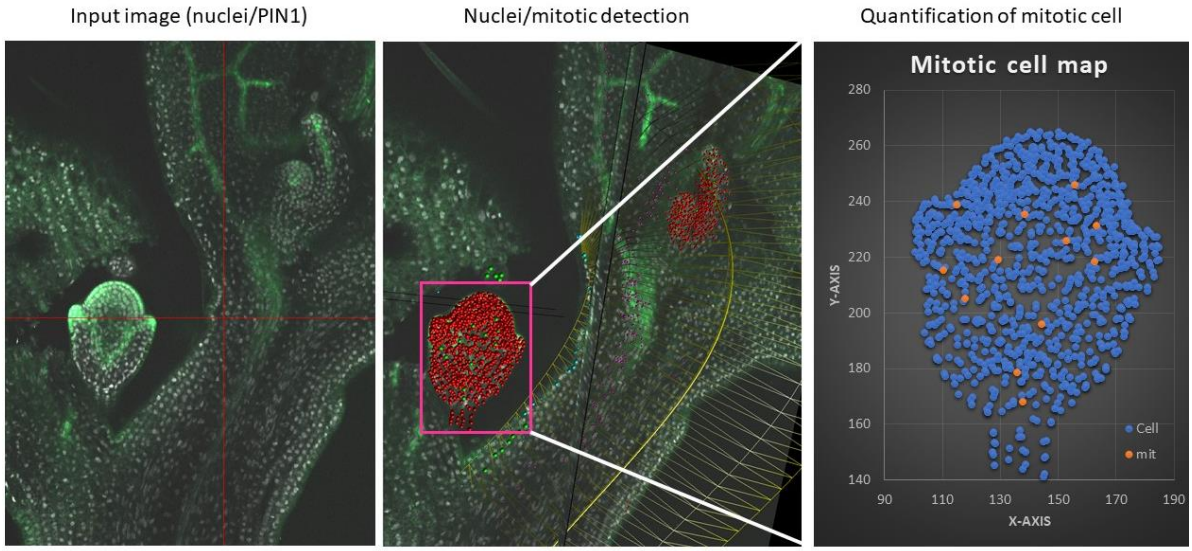

Figure 18. Quantitative analysis of the flower primordia. White- nuclei; Green- PIN1. Mitotic cells are in red (right panel).

Quantification of gene expression localization.

In plants, gene expression occurred cell file/cell position-specific. That's why information about cell type and level of gene expression in each cell is crucial for understanding gene function. The current platform, in combination with previously developed protocols for immune localization (Pasternak et al., 2015) and protein complex detection (proximity ligation assay) (Pasternak et al., 2018), allowed us to perform quantitative analysis of gene expression in each cell and linked it with chromatin status and cell phenotype. These approaches have been used for the analysis of gene expression in several mutants. Here we mentioned PIN1 map with cellular and cell positional resolution and protein proximity in PIN1 overexpression lines.

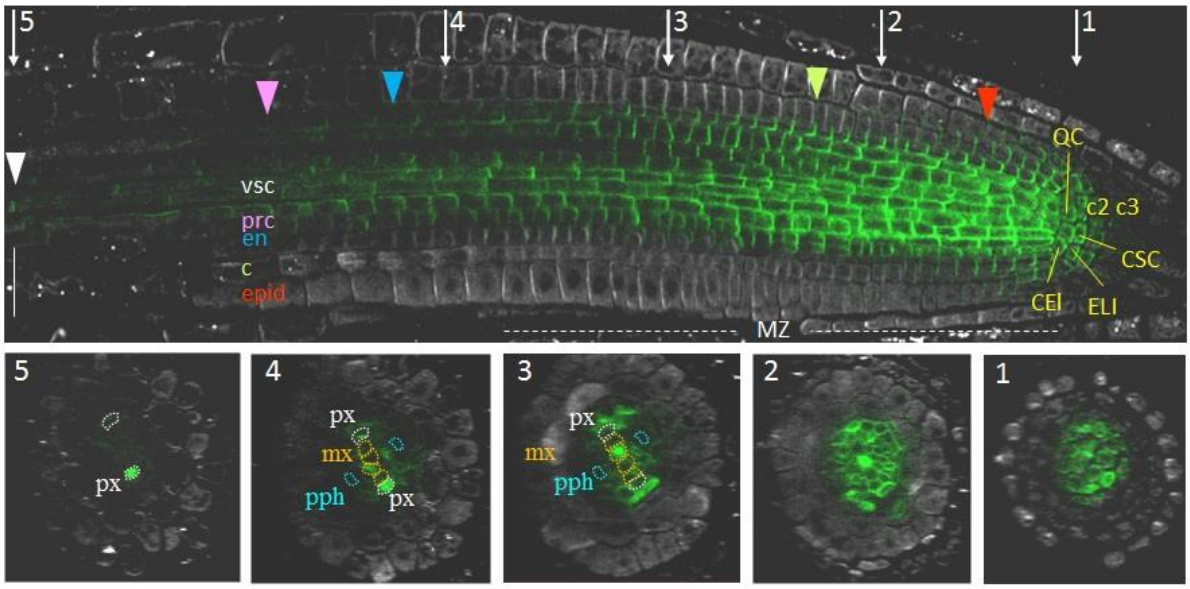

Figure 1. Whole-mount immunolocalisation of PIN1 in *A. thaliana* root tip.

A longitudinal section (above) and five transverse sections (1-5) showing anti-PIN1 signal (green channel) and anti-PIN2 staining (white channel). CEI – cortex/endodermis initials, ELI – epidermis/lateral root cap initials, CSC – columella initials, QC – the quiescent centre, c2 – the second columella tier, c3 – the third columella tier, epid - epidermis, c - cortex, en - endodermis, prc - pericycle, vsc - vasculature, px – protoxylem, pph – protophloem, mx – metaxylem. Coloured triangles - the end of the expression domain in the respective layer. White triangle – rootward PIN1 location in xylem elements in the elongation zone. MZ – the meristematic zone. Bars = 50 µm, from Omelyanchuk et al., 2016.

PIN1 has been detected by immunolocalization. Root have been analysed by the platform. Nuclei were detected, cell file were determined and PIN1 expression patterns were linked with specific cell continuity (files).

Protein complex.

Protein complex abundance is another feature what can be quantify by the platform. Here we present proximity ligation assay what demonstrated formation of protein complex between PIN1 and PIN2 proteins in Arabidopsis root what in turn may abol-

ish PIN's function. The quantitative analysis of PIN1::PIN4 complex were described in Pasternak et al., 2018.

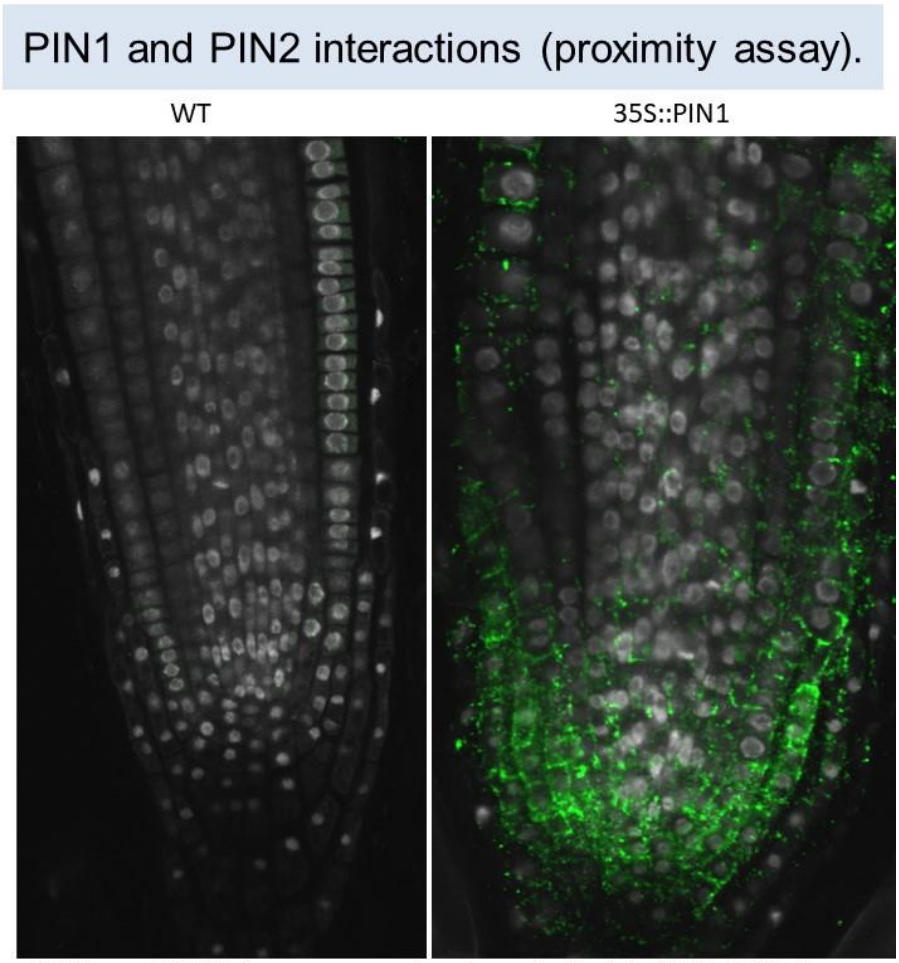

PIN1 and PIN2 form a complex (proximity) in 35S::PIN1 line. Plants have been fixed and subjected to the standard PLA assay. PIN1 anti-mouse and PIN2 anti-rabbit antibody have been used. Protein complex signal is in green, and DAPI is in white.

Literature.

Bassel, G. W. (2019). Multicellular systems biology: quantifying cellular patterning and function in plant organs using network science. *Molecular plant*. Volume 12, ISSUE 6, P731-742, June 03, 2019 DOI:https://doi.org/10.1016/j.molp.2019.02.004

van den Berg C, Willemsen V, Hage W, Weisbeek P, Scheres B (1995) Cell fate in the *Arabidopsis* root meristem determined by directional signalling. Nature 378:62–65

Chen, D. H., Huang, Y., Jiang, C., & Si, J. P. (2018). Chromatin-based regulation of plant root development. *Frontiers in plant science*, *9*, 1509.

Demidchik, V. V., Shashko, A. Y., Bandarenka, U. Y., Smolikova, G. N., Przhevalskaya, D. A., Charnysh, M. A., ... & Yu, M. (2020). Plant Phenomics: Fundamental Bases, Software and Hardware Platforms, and Machine Learning. *Russian Journal of Plant Physiology*, *67*, 397-412.

Emmenlauer, M., Ronneberger, O., Ponti, A., Schwarb, P., Griffa, A., Filippi, A., ... & Burkhardt, H. (2009). XuvTools: free, fast and reliable stitching of large 3D datasets. *Journal of microscopy*, *233*(1), 42-60.

Lavrekha, V. V., Pasternak, T., Ivanov, V. B., Palme, K., & Mironova, V. V. (2017). 3D analysis of mitosis distribution highlights the longitudinal zonation and diarch symmetry in proliferation activity of the Arabidopsis thaliana root meristem. *The Plant Journal*, *92*(5), 834-845.

Kerstens, M., Strauss, S., Smith, R., & Willemsen, V. (2020). From stained plant tissues to quantitative cell segmentation analysis with MorphoGraphX. In *Plant Embryogenesis* (pp. 63-83). Humana, New York, NY.

Kierzkowski, D., Runions, A., Vuolo, F., Strauss, S., Lymbouridou, R., Routier-Kierzkowska, A. L., ... & Zhang, Z. (2019). A growth-based framework for leaf shape development and diversity. *Cell*, *177*(6), 1405-1418.

Kierzkowski, D., & Routier-Kierzkowska, A. L. (2019). Cellular basis of growth in plants: geometry matters. *Current opinion in plant biology*, *47*, 56-63.

Liu, K., Schmidt, T., Blein, T., Dürr, J., Palme, K., & Ronneberger, O. (2013, April). Joint 3d cell segmentation and classification in the arabidopsis root using energy minimization and shape priors. In *2013 IEEE 10th International Symposium on Biomedical Imaging* (pp. 422-425). IEEE.

Liu, K., Lienkamp, S. S., Shindo, A., Wallingford, J. B., Walz, G., & Ronneberger, O. (2014, April). Optical flow guided cell segmentation and tracking in developing tissue. In 2014 IEEE 11th International Symposium on Biomedical Imaging (ISBI) (pp. 298-301). IEEE.

Montenegro-Johnson, T. D., Stamm, P., Strauss, S., Topham, A. T., Tsagris, M., Wood, A. T., ... & Bassel, G. W. (2015). Digital single-cell analysis of plant organ development using 3D CellAtlas. *The Plant Cell*, *27*(4), 1018-1033.

Omelyanchuk, N. A., Kovrizhnykh, V. V., Oshchepkova, E. A., Pasternak, T., Palme, K., & Mironova, V. V. (2016). A detailed expression map of the PIN1 auxin transporter in Arabidopsis thaliana root. *BMC plant biology*, *16*(1), 5.

Pasternak, T., Tietz, O., Rapp, K., Begheldo, M., Nitschke, R., Ruperti, B., & Palme, K. (2015). Protocol: an improved and universal procedure for whole-mount immunolocalization in plants. *Plant Methods*, *11*(1), 50.

Pasternak, T., Haser, T., Falk, T., Ronneberger, O., Palme, K., & Otten, L. (2017). A 3D digital atlas of the Nicotiana tabacum root tip and its use to investigate changes in the root apical meristem induced by the Agrobacterium 6b oncogene. *The Plant Journal*, *92*(1), 31-42.

-
- Pasternak, T., Groot, E. P., Kazantsev, F. V., Teale, W., Omelyanchuk, N., Kovrizhnykh, V., ... & Mironova, V. V. (2019). Salicylic acid affects root meristem patterning via auxin distribution in a concentration-dependent manner. *Plant physiology*, *180*(3), 1725-1739.
- Pasternak, T. P., Ruperti, B., & Palme, K. (2020). A simple high efficiency and low cost in vitro growth system for phenotypic characterization and seed propagation of Arabidopsis thaliana. *bioRxiv*. https://doi.org/10.1101/2020.08.23.263491
-

- Pasternak, T., Teale, W., Falk, T., Ruperti, B., & Palme, K. (2018). A PLA-iRoCS Pipeline for the Localization of Protein–Protein Interactions In Situ. In *Phenotypic Screening* (pp. 161-170). Humana Press, New York, NY.
- de Reuille PB, Routier-Kierzkowska A-L, Kierzkowski D, Bassel GW, Schüpbach T, Tauriello G, Bajpai N, Strauss S, Weber A, Kiss A. 2015. MorphoGraphX: a platform for quantifying morphogenesis in 4D. eLife 4: e05864.
- Savina, M., Lavrekha, V., T Pasternak, Mironova V (2019) Systems biology study on the WOX5 role in the distal part of the root meristem in Arabidopsis thaliana (2019) Plant Genetics, Genomics, Bioinformatics, and Biotechnology (PlantGen2019).
- Schmidt, T., Pasternak, T., Liu, K., Blein, T., Aubry-Hivet, D., Dovzhenko, A., ... & Ronneberger, O. (2014). The iRoCS T oolbox–3 D analysis of the plant root apical meristem at cellular resolution. *The Plant Journal*, *77*(5), 806-814.
- Rowland, R. E., & Nickless, E. M. (2000). Confocal microscopy opens the door to 3-dimensional analysis of cells. *Bioscene*, *26*(3), 3-7.
- Schulz, J., Schmidt, T., Ronneberger, O., Burkhardt, H., Pasternak, T., Dovzhenko, A., & Palme, K. (2006). Fast scalar and vectorial grayscale based invariant features for 3d cell nuclei localization and classification. In *Joint Pattern Recognition Symposium* (pp. 182-191). Springer, Berlin, Heidelberg.

Wolny, A., Cerrone, L., Vijayan, A., Tofanelli, R., Barro, A. V., Louveaux, M., Wenzl C., Steigleder, S., Pape, C., Bailoni, A., Duran-Nebreda S., Bassel, G., Lohmann, J., Hamprecht, F., Schneitz, K., Maizel, A., Kreshuk A., & Duran-Nebreda, S. (2020). Accurate and versatile 3D segmentation of plant tissues at cellular resolution. *BioRxiv*. eLife 2020;9:e57613 doi: 10.7554/eLife.57613

Wunderling, A., Ripper, D., Barra-Jimenez, A., Mahn, S., Sajak, K., Targem, M. B., & Ragni, L. (2018). A molecular framework to study periderm formation in Arabidopsis. *New Phytologist*, *219*(1), 216-229.

Zhu, M., Chen, W., Mirabet, V., Hong, L., Bovio, S., Strauss, S., ... & Li, C. B. (2020). Robust organ size requires robust timing of initiation orchestrated by focused auxin and cytokinin signalling. *Nature Plants*, 1-13.

Supplementary manual:
HRPPP User Manual. The HRPPP user manual, including installation instruction, is written in a tutorial style. The accompanying data sets are available for download on the website (https://lmb.informatik.uni-freiburg.de/lmbsoft/iRoCS/)